Chemical Science

ROYAL SOCIETY OF CHEMISTRY

EDGE ARTICLE

View Article Online
View Journal | View Issue



Cite this: *Chem. Sci.*, 2024, **15**, 15280

All publication charges for this article have been paid for by the Royal Society of Chemistry

Received 11th May 2024
Accepted 14th August 2024

DOI: 10.1039/d4sc03079f

rsc.li/chemical-science



# Visible light photoflow synthesis of a Cu(II) single-chain polymer nanoparticle catalyst†

Sebastian Gillhuber, [abc] Joshua O. Holloway, [bc] Kai Mundsinger, [bc] Jochen A. Kammerer, [bc] Jeffrey R. Harmer, [d] Hendrik Frisch, *[bc] Christopher Barner-Kowollik *[bce] and Peter W. Roesky *[ae]

We herein pioneer the visible light ($\lambda_{max}$ = 410 nm) mediated flow synthesis of catalytically active single-chain nanoparticles (SCNPs). Our design approach is based on a copolymer of poly(ethylene glycol) methyl ether methacrylate and a photocleavable 2-((((2-nitrobenzyl)oxy)carbonyl)amino)ethyl methacrylate monomer which can liberate amine groups upon visible light irradiation, allowing for single-chain collapse *via* the complexation of Cu(II) ions. We initially demonstrate the successful applicability of our design approach for the batch photochemical synthesis of Cu(II) SCNPs and transfer the concept to photoflow conditions, enabling, for the first time, the continuous production of functional SCNPs. Critically, we explore their ability to function as a photocatalyst for the cleavage of carbon–carbon single and double bonds on the examples of xanthene-9-carboxylic acid and oleic acid, demonstrating the advantageous effect SCNPs can provide over analogous small molecule catalysts.

## Introduction

Single-chain nanoparticles (SCNPs) are functional 3D architectures constructed *via* the intramolecular collapse of synthetic macromolecular chains, which mimic the folded state of natural enzymes.[1–5] In recent years, a plethora of approaches have been explored to achieve this intramolecular chain collapse based on covalent[6–20] or non-covalent[21–27] interactions.[2] The folding units can either be randomly distributed along the polymer chain (repeat unit folding) or be located at predefined positions (selective point folding).[4]

Taking inspiration from naturally occurring metalloenzymes, our groups and others have focused on the synthesis of metal functionalized SCNPs, allowing to synergistically combine the tunable characteristics of polymeric materials with the diverse functionalities of metal complexes.[28–43] Exploiting the unique opportunities provided by the SCNP environment in catalytic applications has been a major driving force of the field[44–49] and detailed overviews can be found in the recent literature.[37,50,51]

However, to prevent intermolecular crosslinking throughout SCNP synthesis, the chain folding reactions usually require highly dilute conditions, often significantly below 1 mg mL$^{-1}$,[1] thus limiting the scalability of SCNP synthesis, and consequently the applicability of SCNPs in general. To overcome the scalability problem, flow synthesis – allowing for the continuous production of SCNPs – is highly desirable. In general, flow chemistry has found a variety of applications in organic and polymer synthesis and offers significant advantages in terms of facile scalability and pathways towards commercial production.[52–58] In the realm of SCNPs, the groups of Barner-Kowollik and Diesendruck have demonstrated for the first time how transferring a photochemical batch reaction to photoflow conditions can significantly enhance the efficiency of the process, thereby opening a route to access SCNPs on the gram scale.[58] However, despite the conceivable advantages offered by flow approaches for SCNP synthesis, to the best of our knowledge, no efforts have been undertaken yet to synthesize functional SCNPs under flow conditions.

An ideal system for the flow synthesis of SCNPs allows the mixing of the linear precursor polymer and crosslinker without any immediate initial reaction occurring, thus enabling the simple preparation of one single reaction mixture to be subjected to flow synthesis. During flow synthesis, a suitable trigger must activate either the precursor polymer or the crosslinker,

[a]*Institute of Inorganic Chemistry, Karlsruhe Institute of Technology (KIT), Engesserstraße 15, 76131 Karlsruhe, Germany. E-mail: roesky@kit.edu*
[b]*School of Chemistry and Physics, Queensland University of Technology (QUT), 2 George Street, 4000 Brisbane, QLD, Australia. E-mail: christopher.barnerkowollik@qut.edu.au; h.frisch@qut.edu.au*
[c]*Centre for Materials Science, Queensland University of Technology (QUT), 2 George Street, 4000 Brisbane, QLD, Australia*
[d]*Centre for Advanced Imaging, The University of Queensland (UQ), Building 57 Research Road, 4072 Brisbane, QLD, Australia*
[e]*Institute of Nanotechnology (INT), Karlsruhe Institute of Technology (KIT), Hermann-von-Helmholtz-Platz 1, 76344 Eggenstein-Leopoldshafen, Germany. E-mail: christopher.barner-kowollik@kit.edu*

† Electronic supplementary information (ESI) available: Materials and methods, analytical techniques, action plot analysis, experimental details, analytical data, and catalysis. CCDC 2314460. For ESI and crystallographic data in CIF or other electronic format see DOI: https://doi.org/10.1039/d4sc03079f

thereby inducing the single-chain collapse. While different triggers are conceivable, including but not limited to thermal, electrochemical or photochemical stimuli, our groups are particularly interested in using light to access highly functional tailor-made macromolecular architectures as light efficiently enables high spatiotemporal control over chemical reactions.[59–62]

The single-chain collapse approach usually used for the synthesis of catalytically active, metal-functionalized SCNPs is based on the coordination of Lewis basic functional groups incorporated in the polymer chain to metal cations. To transfer the approach to flow photochemistry, the Lewis basic groups within the linear precursor polymer need to carry protecting groups[63–70] to enable mixing with a metal precursor without any immediate reaction occurring. Thus, a copolymer featuring at least one photobasic comonomer constitutes an ideal system for the photoflow synthesis of metal-functionalized single-chain nanoparticles.

Based on these considerations, we herein target a critical gap in the literature by introducing the first synthesis of catalytically active SCNPs under photoflow conditions. Our design approach is based on a poly(ethylene glycol) methyl ether methacrylate polymer backbone, copolymerized with a photocleavable 2-((((2-nitrobenzyl)oxy)carbonyl)amino)ethyl methacrylate monomer, which can liberate amine groups upon visible light irradiation, allowing single-chain collapse by complexation of Cu(II) ions *via* the liberated amines. Initially, we investigate the photochemical response of the photolabile monomer following our well-established photochemical action plot methodology.[71,72] Based on the insights gained from the action plot, we show the successful applicability of our concept in batch SCNP synthesis and subsequently demonstrate its transferability to flow conditions using a commercially available photoflow reactor. Critically, we explore the catalytic performance of the resulting Cu(II) SCNPs for the visible light photocatalyzed cleavage of C–C single and double bonds on the examples of xanthene-9-carboxylic acid and oleic acid, demonstrating the advantageous effect the SCNP environment can provide compared to similar small molecule catalysts.

## Results and discussion

### Monomer photochemical action plot

We initially probed the wavelength dependent cleavage response of the literature-known monomer 2-((((2-nitrobenzyl)oxy)carbonyl)amino)ethyl methacrylate, which can liberate Lewis basic amine groups upon light irradiation,[73–75] *via* our photochemical action plot methodology.[71,72] While the photochemical behaviour of a monomeric system is not necessarily identical to its polymeric counterpart, the investigation of the monomer can still provide valuable insights.[76] The photochemical action plot obtained for 2-((((2-nitrobenzyl)oxy)carbonyl)amino) ethyl methacrylate in acetonitrile in the wavelength range between 230 nm and 440 nm is shown in Fig. 1 (refer to ESI Chapter 3† for details).

It is evident that the wavelength dependent reactivity pattern is red-shifted by about 50 nm compared to the extinction

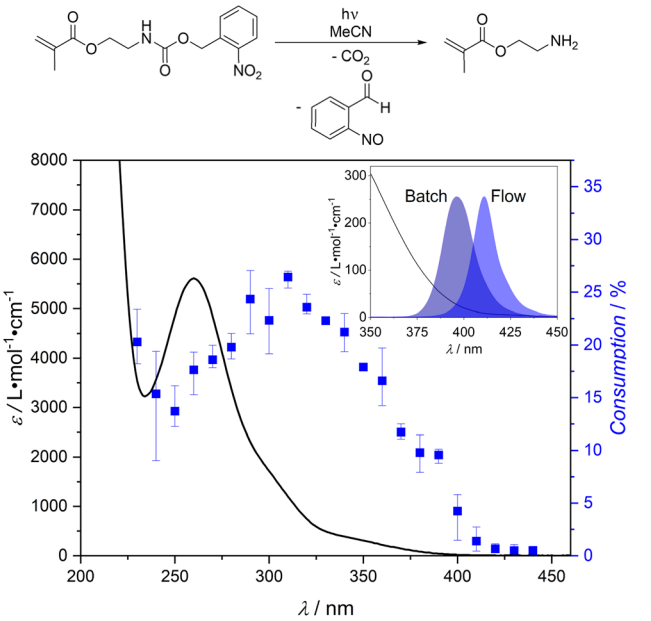


Fig. 1 Photochemical action plot of the photocleavage of 2-((((2-nitrobenzyl)oxy)carbonyl)amino)ethyl methacrylate to 2-aminoethyl methacrylate in acetonitrile at a concentration of 0.5 mg $mL^{-1}$, showing the consumption of the starting material upon irradiation with the same number of photons ($1.99 \times 10^{18}$ photons) at different wavelengths. Error bars indicate the lowest and highest determined conversion at each wavelength, respectively. Details regarding the photochemical action plot methodology are given in the ESI (Chapter 3).† The insert shows the extinction at high wavelengths, superimposed with the emission spectra of the LEDs employed for the batch and flow synthesis of SCNPs within the current work.

maximum of 2-((((2-nitrobenzyl)oxy)carbonyl)amino)ethyl methacrylate, an observation previously made for *ortho*-nitrobenzyl photocleavage reactions.[76,77] Usually, photochemical action plots are employed to determine the wavelength of maximum photoreaction efficiency, which is often strongly disparate from the absorption maximum observed in a UV/vis spectrum.[71,72] In the current case, we were additionally intrigued by the finding that reactivity was still observed at wavelengths above 400 nm, where the extinction coefficient is significantly below 100 L $mol^{-1}$ $cm^{-1}$ (refer to Fig. 1), indicating that visible light can be employed for the cleavage of our photolabile protecting group.

### SCNP batch synthesis

To incorporate the photolabile monomer into a polymer, it was copolymerized with poly(ethylene glycol) methyl ether methacrylate (average $M_n$ = 300 g $mol^{-1}$) *via* reversible addition–fragmentation chain-transfer (RAFT) polymerization,[78] resulting in polymer **P1** (refer to Fig. 2). Size exclusion chromatography (SEC) in tetrahydrofuran (THF) gave an indication of the number-averaged molar mass ($M_n$) of $M_n$ = 28 200 g $mol^{-1}$ and dispersity ($Đ$) of $Đ$ = 1.2. Employing $^1$H nuclear magnetic resonance (NMR) spectroscopy, a content of approximately 14% of incorporated photolabile monomer was determined, in good agreement with the monomer feed ratio (refer to ESI Chapters

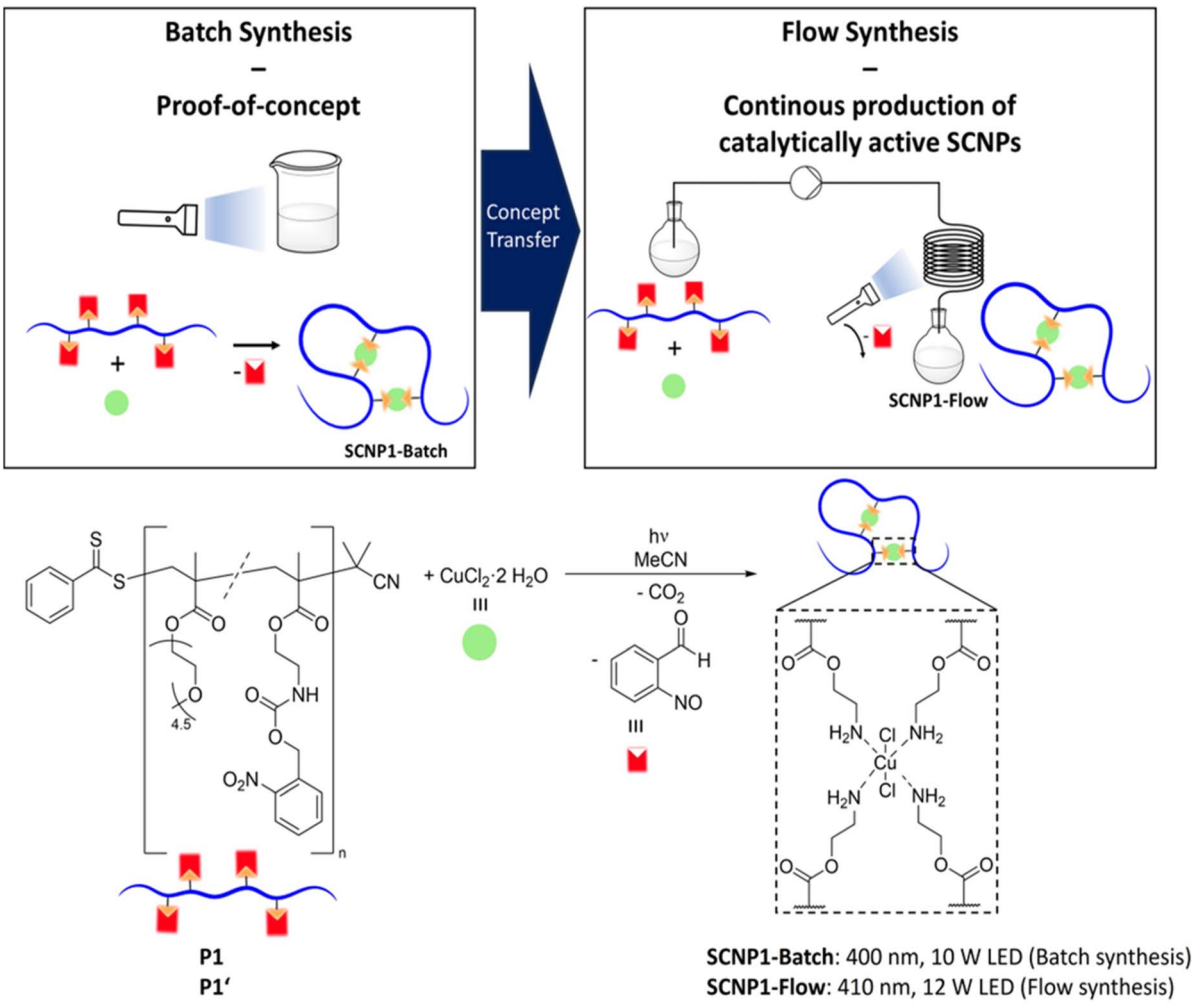


Fig. 2 (Top) Schematic illustration of generating functional single-chain nanoparticles (SCNPs) *via* batch and flow synthesis. A linear precursor polymer featuring photobasic amine groups is irradiated in the presence of Cu(II) ions, forming catalytically active Cu(II) SCNPs. Transferring the concept from a batch photochemical process to photoflow conditions allows – in principle – for their continuous production. (Bottom) Reaction scheme for the synthesis of Cu(II) SCNPs. **SCNP1-Batch** is prepared in a batch photochemical process from the linear precursor polymer **P1**, **SCNP1-Flow** from a second batch of the same polymer (**P1′**) under photoflow conditions. The depiction of the SCNP folding unit is based on a model complex (refer to ESI Fig. S28†).

4.1 and 4.2†). The targeted polymer is a statistical copolymer; therefore, SCNP folding reactions reported herein follow the repeat unit approach.[4]

To prove that the developed methodology of using a polymer with photobasic functional groups combines access to metal-functionalized SCNPs with temporal control over the folding process, **P1** was mixed with copper(II) chloride dihydrate in acetonitrile at a polymer concentration of 2 mg $mL^{-1}$ and irradiated using a light-emitting diode (LED, centred at 400 nm, refer to Fig. 1 for emission spectrum) in a batch process, resulting in **SCNP1-Batch**.

$^1$H NMR spectroscopy indicated the quantitative deprotection of the linear precursor polymer by disappearance of the resonances associated with the photolabile *ortho*-nitrobenzyl group at $\delta = 8.20$–$7.45$ ppm, 6.35–6.15 ppm and 5.52–5.38 ppm (refer to insert in Fig. 3a). As $^1$H NMR spectroscopy is incapable of differentiating the desired intrachain collapse from undesirable interchain crosslinking, size sensitive techniques were employed to follow the SCNP folding reaction. Comparing the size distributions of **P1** and **SCNP1-Batch** obtained *via* SEC in THF shows that the entire distribution of the latter is shifted towards later retention times, indicating a decrease in the solvodynamic volume, thus validating successful SCNP compaction (refer to Fig. 3c). We note, however, that additional experiments indicated potential enthalpic interactions of the SCNP sample, depending on the SEC columns. To corroborate the observed compaction, dynamic light scattering (DLS) measurements in acetonitrile were conducted, evidencing a decrease in the solvodynamic diameter ($D_h$), derived from the number-averaged size distributions, from $D_h = 6.4$ nm for **P1** to $D_h = 3.1$ nm for **SCNP1-Batch** (refer to Fig. 3d), in line with SCNP compaction. We note in passing that DLS data of particles of such small diameters need to be treated with caution due to their low scattering abilities.[5] Diffusion-ordered $^1$H NMR

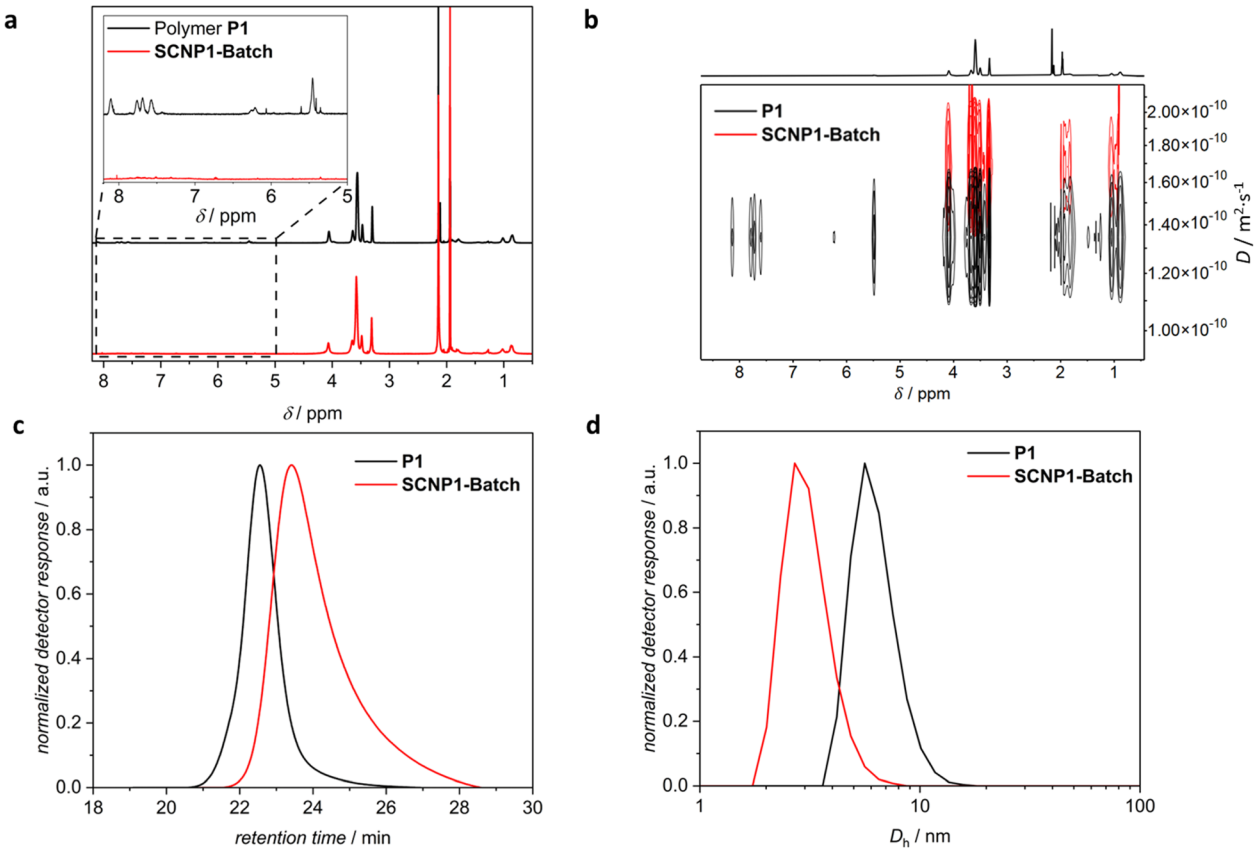


Fig. 3 (a) $^{1}$H NMR spectra (600 MHz, $CD_3CN$, 298 K, refer to ESI Chapter 4† for resonance assignments), (b) DOSY NMR spectra (400 MHz, $CD_3CN$, 301 K), (c) SEC chromatograms (THF, RI), and (d) number-weighted DLS size distributions ($CH_3CN$) of polymer **P1** (black) and **SCNP1-Batch** (red).

spectroscopy (DOSY) measurements in $CD_3CN$ showed an increase in the diffusion coefficient from $1.43 \times 10^{-10}$ m$^2$ s$^{-1}$ for **P1** to $1.71 \times 10^{-10}$ m$^2$ s$^{-1}$ for **SCNP1-Batch** (refer to Fig. 3b), again in line with the desired SCNP compaction.

Additional control reactions indicate that the simultaneous presence of both $CuCl_2 \cdot 2H_2O$ and light is critical for the successful formation of **SCNP1-Batch** (refer to ESI Fig. S4†) and that **P1** is stable under ambient light conditions and only deprotected under high-intensity LED irradiation (refer to ESI Fig. S2†).

To obtain a more detailed understanding of the structure of the actual SCNP folding unit, a small molecule model complex was synthesized. For that, 2-phenylethylamine was chosen as a small molecule mimic of the ethylamine moieties liberated after cleavage of the *ortho*-nitrobenzyl protecting groups upon irradiation of **P1**. The mixing of 2-phenylethylamine with $CuCl_2 \cdot 2H_2O$ in acetonitrile resulted in the hexa-coordinated complex [(2-phenylethylamine)$_4$CuCl$_2$] depicted in ESI Fig. S28.† The central copper ion is coordinated by four amine ligands in a square planar fashion and additionally by two chloride ions, resulting in a Jahn–Teller distorted octahedron, as expected for the d$^9$ ion Cu(II).[79] We note, however, that the coordination environment within our Cu(II) folded SCNP may differ from that observed in the model complex due to flexibility constraints within the polymer framework and the presence of additional oxygen atoms. Nonetheless, the model complex unambiguously evidences the capability of ethylamine based ligand systems to bind to Cu(II) ions under the conditions employed in the synthesis of **SCNP1-Batch**.

## SCNP flow synthesis

Building on these successful results, we prepared a new batch of polymer (**P1′**) analogously to **P1** for exploration of SCNP synthesis in flow. SEC measurements of **P1′** in THF indicated a number-averaged molar mass of $M_n = 30\,900$ g mol$^{-1}$ and dispersity of $Đ = 1.2$. Using $^{1}$H NMR spectroscopy, the amount of photolabile functional groups within the copolymer was estimated to be approximately 15% (refer to ESI Chapters 4.1 and 4.2†).

Employing a commercially available photoflow reactor (Vapourtec E-series, refer to ESI Chapter 2.7† for details), a mixture of **P1′** and $CuCl_2 \cdot 2H_2O$ in acetonitrile was subjected to irradiation with a 410 nm LED (12 W, refer to Fig. 1 for emission spectrum) under flow conditions at a flow rate of 0.2 mL min$^{-1}$ and a polymer concentration of 2 mg mL$^{-1}$. The tubing volume exposed to light in the photoflow process is 10 mL, resulting in a total irradiation time of 50 minutes, which is similar to the time necessary for the complete deprotection of **P1** under batch conditions (refer to ESI Fig. S3†). The complete deprotection of polymer **P1′** during the photoflow reaction is

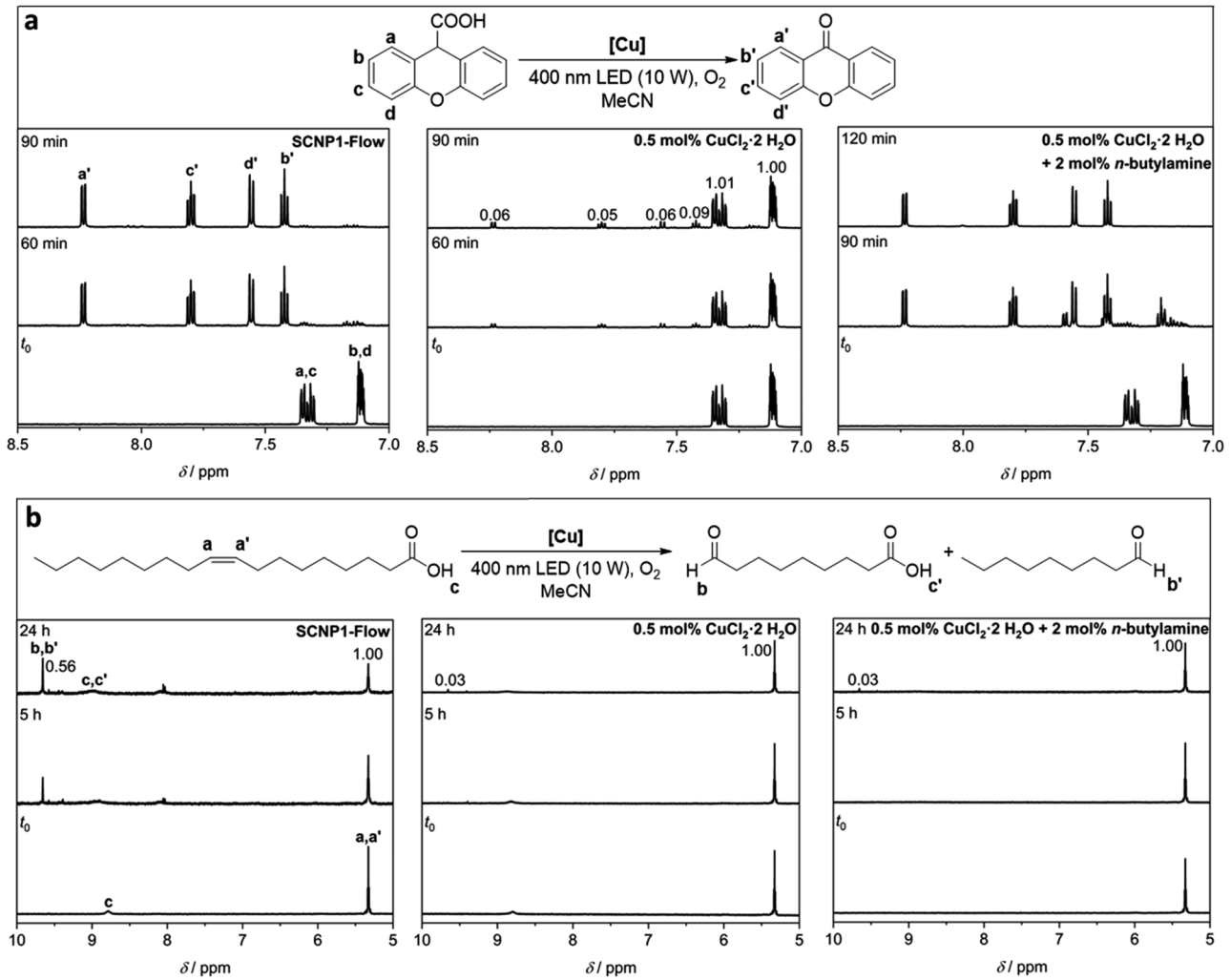


Fig. 4 Reaction schemes and $^1$H NMR spectra (600 MHz, $CD_3CN$, 298 K) of (a) the photocatalytic decarboxylation and oxygenation of xanthene-9-carboxylic acid and (b) the oxidative cleavage of oleic acid employing **SCNP1-Flow** (left), $CuCl_2 \cdot 2H_2O$ (centre) or $CuCl_2 \cdot 2H_2O$ in the presence of *n*-butylamine (right) as the catalyst. Resonance labels refer to the respective schemes above the spectra. Numbers on resonances denote integral values.

evident from $^1$H NMR spectroscopy (refer to ESI Fig. S13†). The resulting **SCNP1-Flow** was analysed by SEC in THF, showing a shift of the entire molar mass distribution of **SCNP1-Flow** towards later retention times compared to that of **P1′**, evidencing successful SCNP compaction (refer to ESI Fig. S18†). SCNP folding was additionally verified by DLS (refer to ESI Fig. S21†), evidencing a decrease in the solvodynamic diameter from $D_h = 6.7$ nm for **P1′** to $D_h = 4.7$ nm for **SCNP1-Flow**, and DOSY (refer to ESI Fig. S23 and S25†), showing an increase in the diffusion coefficient from $1.47 \times 10^{-10}$ m$^2$ s$^{-1}$ for **P1′** to $1.56 \times 10^{-10}$ m$^2$ s$^{-1}$ for **SCNP1-Flow**. A comparison of the size data to that of **SCNP1-Batch** is provided in ESI Chapter 5.10.†

To remove any unreacted $CuCl_2 \cdot 2H_2O$ from the reaction mixture, the solution obtained after the photoflow process was subjected to purification by preparative SEC (refer to ESI Chapter 4.5† for details). The integrity of the polymer during this purification process was verified by SEC measurements in THF (refer to ESI Fig. S18†), and energy dispersive X-ray spectroscopy (EDX) confirmed that Cu is still present in the polymer (refer to ESI Fig. S26†). The actual metal content within **SCNP1-Flow** was quantified using electron paramagnetic resonance (EPR) spectroscopy (refer to ESI Chapter 5.9† for details). An average Cu(II) concentration in solutions of **SCNP1-Flow** of about 0.05 mmol L$^{-1}$ was determined.

To the best of our knowledge, our concept constitutes the first example of a metal functionalized SCNP synthesized under flow conditions. We note that the scalability of the approach presented herein is limited as increasing the polymer concentration or flow rate leads to incomplete deprotection of **P1′** and unidentified side reactions (refer to ESI Chapter 4.5†). Nevertheless, the flow approach enables the simple and continuous production of any desired quantity of **SCNP1-Flow**. Contrary, a batch process would be limited by (i) the difficulty to ensure a homogeneous light distribution through large sample volumes and (ii) the alternative – running several batch reactions in a row – would constitute a time-consuming and inefficient effort.

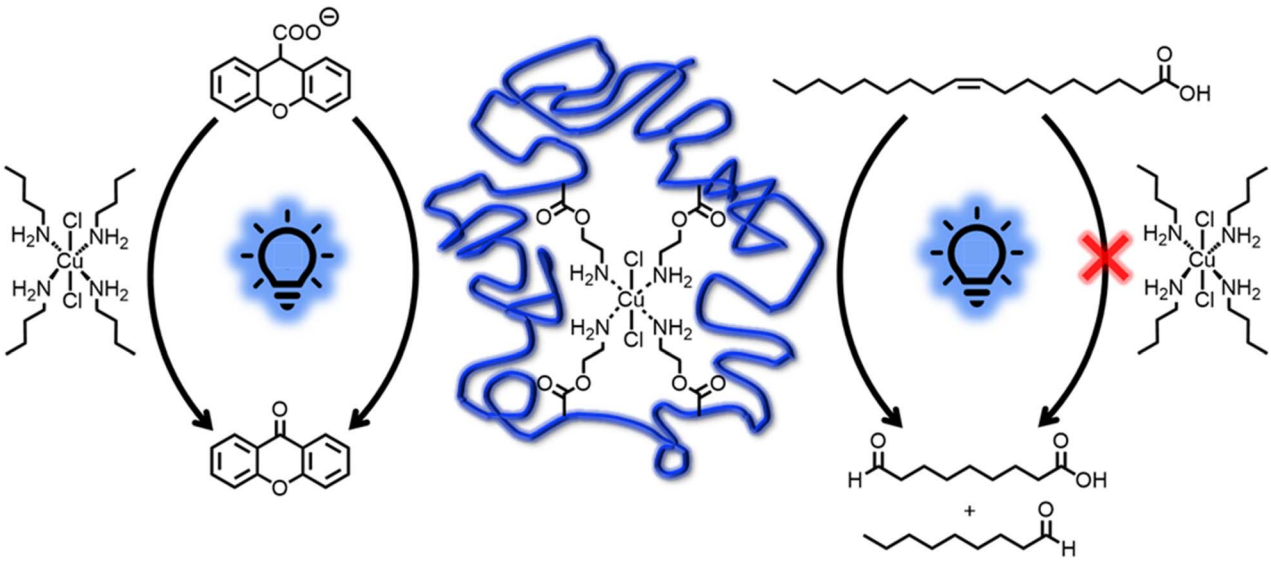

Fig. 5 Graphical illustration of the stabilizing effect that the polymeric environment of SCNP1-Flow provides for the catalytically active moiety. While the photocatalytic decarboxylation and oxygenation of xanthene-9-carboxylic acid (left) is catalyzed by SCNP1-Flow as well as tetra(*n*-butylamine) copper(II) chloride, the latter is inactive in the oxidative cleavage of oleic acid (**right**).

## Catalysis

Having the Cu(II) functionalized **SCNP1-Flow** at hand, we employed them for the Cu-catalyzed photocatalytic cleavage of C–C bonds, as recently demonstrated by the groups of Lee and Jiang.[80] Specifically, we focused on the decarboxylation-oxygenation of xanthene-9-carboxylic acid and the oxidative double bond cleavage of oleic acid (refer to Fig. 4) as we found these reactions to occur without the formation of side products, thus enabling convenient tracking of the reaction progress *via* NMR spectroscopy. The yields obtained in the individual reactions are summarized in ESI Table S12.† At first, the substrates, either xanthene-9-carboxylic acid or oleic acid, respectively, were irradiated with a 400 nm LED (10 W, refer to Fig. 1 for emission spectrum) in the presence of catalytic amounts of **SCNP1-Flow** (about 0.5 mol% Cu(II), refer to ESI Chapter 5.9†) under oxygen atmosphere. These catalytic reactions were performed in triplicate (refer to ESI Chapter 6†). Control reactions ensured that the presence of **SCNP1-Flow** is critical and that neither LED irradiation alone nor the presence of **P1′** itself combined with LED irradiation catalyze the product formation. Additional control reactions demonstrate the necessity of light irradiation and prove that purification by preparative SEC efficiently removes unreacted $CuCl_2 \cdot 2H_2O$ after SCNP synthesis (refer to ESI Chapter 6† for all control reactions).

For xanthene-9-carboxylic acid, a quantitative conversion to 9-xanthenone within 90 minutes was observed *via* $^1$H NMR spectroscopy (refer to Fig. 4a and ESI Fig. S36–S38†). For the oxidative cleavage of the double bond of oleic acid to nonanal and 9-oxononanoic acid, a conversion close to 40% within 24 hours was observed *via* $^1$H NMR spectroscopy (refer to Fig. 4b and ESI Fig. S53–S55†). Increased irradiation times (up to three days) led to a maximum conversion of approximately 50% (refer to ESI Fig. S55†). The same results were obtained when **SCNP1-Batch** was employed as the catalyst (refer to ESI Fig. S52 and S70†).

It is well established that the specific environment of the active catalyst within SCNPs can offer advantages over analogue small molecule catalysts.[37,50,81–84] Indeed, conducting the catalytic reactions with 0.5 mol% of $CuCl_2 \cdot 2H_2O$ instead of **SCNP1-Flow** resulted in a significantly lower rate of the catalytic transformations. For xanthene-9-carboxylic acid, only a conversion of about 10% was observed within 90 minutes (refer to Fig. 4a and ESI Fig. S39–S41†), in contrast to quantitative conversion when **SCNP1-Flow** is employed. Similarly, for oleic acid a conversion of less than 5% was observed after 24 hours (refer to Fig. 4b and ESI Fig. S56–S58†), compared to about 40% for **SCNP1-Flow**. To achieve reaction rates similar to those observed for **SCNP1-Flow**, the $CuCl_2 \cdot 2H_2O$ load had to be increased 20-fold to 10 mol% (refer to ESI Fig. S42–S44 and S59–S61†).

To rationalize the reason for the drastic difference in catalytic performance between **SCNP1-Flow** and $CuCl_2 \cdot 2H_2O$, additional experiments were performed. The characteristic differences between these two catalysts are (i) the presence of a polymeric environment and (ii) the coordination of amine groups to the Cu ions within **SCNP1-Flow**, which are both absent for $CuCl_2 \cdot 2H_2O$. To investigate whether the presence of the polymer plays an important role, a homopolymer of poly(ethylene glycol) methyl ether methacrylate (poly(PEGMEMA)), mimicking the polymer backbone of **SCNP1-Flow**, was synthesized. Running the catalytic reactions at a catalyst load of 0.5 mol% $CuCl_2 \cdot 2H_2O$ in the presence of this polymer did not affect the rate of the catalytic reactions (refer to ESI Fig. S50 and S68†).

To mimic the coordination of the Cu ions by primary amine moieties within **SCNP1-Flow**, the catalytic reactions were conducted again with 0.5 mol% $CuCl_2 \cdot 2H_2O$ in the presence of

2 mol% *n*-butylamine. For xanthene-9-carboxylic acid, this resulted in a drastic increase in the catalytic rate compared to $CuCl_2 \cdot 2H_2O$ itself, and the reaction was completed within 120 minutes (refer to Fig. 4a and ESI Fig. S51†). This clearly shows that the coordination environment of the Cu ions plays a key role and rationalizes the drastic differences in catalytic performance between **SCNP1-Flow** and $CuCl_2 \cdot 2H_2O$. In contrast, for oleic acid, no such effect was observed (refer to Fig. 5) and running the reactions with $CuCl_2 \cdot 2H_2O$ in the presence of *n*-butylamine did not increase the rate of the catalytic reaction (refer to Fig. 4b and ESI Fig. S69†). Instead, the presence of *n*-butylamine led to the deprotonation of oleic acid as is evident from the disappearance of the carboxylic acid proton resonance at $\delta = 8.90$–$8.70$ ppm in the $^1$H NMR spectrum of this reaction mixture (refer to Fig. 4b and ESI Fig. S69†). In contrast, when **SCNP1-Flow** is employed as the catalyst, no deprotonation of oleic acid by the polymer bound amines is observed as is evident from the presence of the carboxylic acid proton resonance at $\delta =$ 8.90–8.70 ppm in the $^1$H NMR spectra of the corresponding reactions (refer to Fig. 4b and ESI Fig. S53–S55†). It thus seems plausible that the amines remain bonded to the Cu ions, exerting their advantageous effect on the catalytic rate, rationalizing the observed substantial increase in catalytic performance of **SCNP1-Flow** with respect to $CuCl_2 \cdot 2H_2O$.

A rigorous rationalization of these findings would require precise knowledge of the p$K_a$ values of all species present in the reaction solutions. Based on the literature,[85–88] the situation in acetonitrile is considerably different from that in aqueous solution and strongly depends on delicate equilibria. Further complications may arise from self-assembly or micelle formation upon deprotonation of oleic acid.[89] These considerations render an in-depth investigation of the observations challenging and beyond the scope of the current study. Nonetheless, our results demonstrate that shielding the catalytic entity within the SCNP environment has a critical and positive effect on catalysis, enabling reactivities unachievable with analogue small molecule catalysts.

## Conclusions

In summary, we pioneer the visible light mediated photoflow synthesis of catalytically active Cu(II) folded single-chain nanoparticles (SCNPs). Specifically, we investigate the wavelength-resolved reactivity of the photolabile 2-((((2-nitrobenzyl)oxy) carbonyl)amino)ethyl methacrylate monomer and employ it for the synthesis of a poly(ethylene glycol) methyl ether methacrylate copolymer featuring photobasic amine groups. Visible light irradiation of the resulting photolabile polymer in the presence of copper(II) chloride dihydrate in a batch photochemical process gives access to **SCNP1-Batch**, constituting the first example of visible-light mediated metal-induced SCNP compaction. Building on these proof-of-concept results, we transfer our chemical approach to a commercially available photoflow reactor, enabling the continuous synthesis of **SCNP1-Flow**. We demonstrate the activity of the latter in the photocatalytic cleavage of carbon–carbon single and double bonds on the examples of xanthene-9-carboxylic acid and oleic acid, highlighting the advantageous effects the SCNP environment can provide over analogous small molecule catalysts. Our study paves the way for future flow synthetic approaches to the continuous production of functional SCNPs. Critically, our study serves as inspiration for the design of tailor-made catalytic pockets, enabling reactivities unachievable with small molecule catalysts.

## Data availability

Experimental data is available in the ESI.† All synthetic protocols, spectroscopic data, supplementary figures and tables, and detailed crystallographic information can be found in the ESI.† Crystallographic data are available *via* the Cambridge Crystallographic Data Centre (CCDC): 2314460.†

## Author contributions

S. G.: conceptualization, methodology, formal analysis, investigation, writing – original draft, review & editing, visualization, project administration, J. O. H.: conceptualization, writing – review & editing, supervision, project administration, K. M.: writing – review & editing, resources, J. A. K.: investigation (EDX), writing – review & editing, J. R. H.: investigation (EPR), writing – review & editing, H. F.: conceptualization, writing – review & editing, supervision, project administration, C. B.-K.: conceptualization, writing – review & editing, supervision, project administration, funding acquisition, P. W. R.: conceptualization, writing – review & editing, supervision, project administration, funding acquisition.

## Conflicts of interest

There are no conflicts to declare.

## Acknowledgements

S. G. acknowledges funding by the Fonds der Chemischen Industrie in the form of a Kekulé followship (No. 110160). C. B.-K. and H. F. acknowledge the Australian Research Council (ARC) for a Laureate and DECRA Fellowship, respectively. C. B.-K. and H. F. acknowledge continuous support by QUT's Centre for Materials Science. J. A. K. acknowledges the Deutsche Forschungsgemeinschaft (DFG, German Research Foundation) for his WBP fellowship (500289223). J. R. H. thanks the ARC for funding (LE230100048). All authors acknowledge QUT's Central Analytical Research Facility (CARF) supported by QUT's Research Portfolio. Dr Joshua Carroll (QUT) is acknowledged for support with the photochemical action plot related infrastructure. Dr Lewis Chambers (QUT) is acknowledged for the measurement of LED emission spectra. Fred Pashley-Johnson (QUT/Ghent University) is acknowledged for support with LCMS measurements. A/Prof. James Blinco (QUT) and Nicholas Roxburgh (QUT) are acknowledged for support with EPR experiments. Dr Patrick Maag (QUT/KIT) is acknowledged for fruitful discussions. Sibylle Schneider (KIT) and Dr Cedric

 

Uhlmann (KIT) are thanked for performing and analyzing single crystal X-ray diffraction experiments.

## References

1 A. M. Hanlon, C. K. Lyon and E. B. Berda, What is next in single-chain nanoparticles?, *Macromolecules*, 2016, **49**, 2–14.
2 C. K. Lyon, A. Prasher, A. M. Hanlon, B. T. Tuten, C. A. Tooley, P. G. Frank and E. B. Berda, A brief user's guide to single-chain nanoparticles, *Polym. Chem.*, 2015, **6**, 181–197.
3 O. Altintas and C. Barner-Kowollik, Single chain folding of synthetic polymers by covalent and non-covalent interactions: current status and future perspectives, *Macromol. Rapid Commun.*, 2012, **33**, 958–971.
4 O. Altintas and C. Barner-Kowollik, Single-chain folding of synthetic polymers: a critical update, *Macromol. Rapid Commun.*, 2016, **37**, 29–46.
5 E. Blasco, B. T. Tuten, H. Frisch, A. Lederer and C. Barner-Kowollik, Characterizing single chain nanoparticles (SCNPs): a critical survey, *Polym. Chem.*, 2017, **8**, 5845–5851.
6 E. Harth, B. Van Horn, V. Y. Lee, D. S. Germack, C. P. Gonzales, R. D. Miller and C. J. Hawker, A facile approach to architecturally defined nanoparticles *via* intramolecular chain collapse, *J. Am. Chem. Soc.*, 2002, **124**, 8653–8660.
7 A. Tuteja, M. E. Mackay, C. J. Hawker, B. Van Horn and D. L. Ho, Molecular architecture and rheological characterization of novel intramolecularly crosslinked polystyrene nanoparticles, *J. Polym. Sci., Part B: Polym. Phys.*, 2006, **44**, 1930–1947.
8 J. N. Dobish, S. K. Hamilton and E. Harth, Synthesis of low-temperature benzocyclobutene cross-linker and utilization, *Polym. Chem.*, 2012, **3**, 857–860.
9 T. E. Dukette, M. E. Mackay, B. Van Horn, K. L. Wooley, E. Drockenmuller, M. Malkoch and C. J. Hawker, Conformation of intramolecularly cross-linked polymer nanoparticles on solid substrates, *Nano Lett.*, 2005, **5**, 1704–1709.
10 O. Altintas, J. Willenbacher, K. N. R. Wuest, K. K. Oehlenschlaeger, P. Krolla-Sidenstein, H. Gliemann and C. Barner-Kowollik, A mild and efficient approach to functional single-chain polymeric nanoparticles *via* photoinduced diels-alder ligation, *Macromolecules*, 2013, **46**, 8092–8101.
11 I. Perez-Baena, I. Loinaz, D. Padro, I. Garcia, H. J. Grande and I. Odriozola, Single-chain polyacrylic nanoparticles with multiple Gd(III) centres as potential MRI contrast agents, *J. Mater. Chem.*, 2010, **20**, 6916–6922.
12 A. R. de Luzuriaga, N. Ormategui, H. J. Grande, I. Odriozola, J. A. Pomposo and I. Loinaz, Intramolecular click cycloaddition: an efficient room-temperature route towards bioconjugable polymeric nanoparticles, *Macromol. Rapid Commun.*, 2008, **29**, 1156–1160.
13 N. Ormategui, I. Garcia, D. Padro, G. Cabanero, H. J. Grande and I. Loinaz, Synthesis of single chain thermoresponsive polymer nanoparticles, *Soft Matter*, 2012, **8**, 734–740.
14 A. R. de Luzuriaga, I. Perez-Baena, S. Montes, I. Loinaz, I. Odriozola, I. Garcia and J. A. Pomposo, New route to polymeric nanoparticles by click chemistry using bifunctional cross-linkers, *Macromol. Symp.*, 2010, **296**, 303–310.
15 H. Frisch, J. P. Menzel, F. R. Bloesser, D. E. Marschner, K. Mundsinger and C. Barner-Kowollik, Photochemistry in confined environments for single-chain nanoparticle design, *J. Am. Chem. Soc.*, 2018, **140**, 9551–9557.
16 A. E. Cherian, F. C. Sun, S. S. Sheiko and G. W. Coates, Formation of nanoparticles by intramolecular cross-linking: following the reaction progress of single polymer chains by atomic force microscopy, *J. Am. Chem. Soc.*, 2007, **129**, 11350–11351.
17 A. Sanchez-Sanchez, D. A. Fulton and J. A. Pomposo, pH-responsive single-chain polymer nanoparticles utilising dynamic covalent enamine bonds, *Chem. Commun.*, 2014, **50**, 1871–1874.
18 L. Buruaga and J. A. Pomposo, Metal-free polymethyl methacrylate (PMMA) nanoparticles by enamine "click" chemistry at room temperature, *Polymers*, 2011, **3**, 1673–1683.
19 J. B. Beck, K. L. Killops, T. Kang, K. Sivanandan, A. Bayles, M. E. Mackay, K. L. Wooley and C. J. Hawker, Facile preparation of nanoparticles by intramolecular cross-linking of isocyanate functionalized copolymers, *Macromolecules*, 2009, **42**, 5629–5635.
20 J. G. Wen, L. Yuan, Y. F. Yang, L. Liu and H. Y. Zhao, Self-assembly of monotethered single-chain nanoparticle shape amphiphiles, *ACS Macro Lett.*, 2013, **2**, 100–106.
21 O. Altintas, E. Lejeune, P. Gerstel and C. Barner-Kowollik, Bioinspired dual self-folding of single polymer chains *via* reversible hydrogen bonding, *Polym. Chem.*, 2012, **3**, 640–651.
22 O. Altintas, T. Rudolph and C. Barner-Kowollik, Single chain self-assembly of well-defined heterotelechelic polymers generated by ATRP and click chemistry revisited, *J. Polym. Sci., Part A: Polym. Chem.*, 2011, **49**, 2566–2576.
23 O. Altintas, P. Gerstel, N. Dingenouts and C. Barner-Kowollik, Single chain self-assembly: preparation of alpha, omega-donor–acceptor chains *via* living radical polymerization and orthogonal conjugation, *Chem. Commun.*, 2010, **46**, 6291–6293.
24 J. C. Nelson, J. G. Saven, J. S. Moore and P. G. Wolynes, Solvophobically driven folding of nonbiological oligomers, *Science*, 1997, **277**, 1793–1796.
25 D. D. Prabhu, K. Aratsu, Y. Kitamoto, H. Ouchi, T. Ohba, M. J. Hollamby, N. Shimizu, H. Takagi, R. Haruki, S. I. Adachi and S. Yagai, Self-folding of supramolecular polymers into bioinspired topology, *Sci. Adv.*, 2018, **4**, eaat8466.
26 P. Wu, A. Pietropaolo, M. Fortino, S. Shimoda, K. Maeda, T. Nishimura, M. Bando, N. Naga and T. Nakano, Non-uniform self-folding of helical poly(fluorenevinylene) derivatives in the solid state leading to amplified circular dichroism and circularly polarized light emission, *Angew. Chem., Int. Ed.*, 2022, **61**, e202210556.

27 R. S. Lokey and B. L. Iverson, Synthetic molecules that fold into a pleated secondary structure in solution, *Nature*, 1995, **375**, 303–305.
28 J. L. Bohlen, B. Kulendran, H. Rothfuss, C. Barner-Kowollik and P. W. Roesky, Heterobimetallic Au(I)/Y(III) single chain nanoparticles as recyclable homogenous catalysts, *Polym. Chem.*, 2021, **12**, 4016–4021.
29 S. Gillhuber, J. O. Holloway, H. Frisch, F. Feist, F. Weigend, C. Barner-Kowollik and P. W. Roesky, Ferrocene-driven single-chain polymer compaction, *Chem. Commun.*, 2023, **59**, 4672–4675.
30 A. E. Izuagbe, V. X. Truong, B. T. Tuten, P. W. Roesky and C. Barner-Kowollik, Visible light switchable single-chain nanoparticles, *Macromolecules*, 2022, **55**, 9242–9248.
31 P. H. Maag, F. Feist, H. Frisch, P. W. Roesky and C. Barner-Kowollik, Fluorescent and catalytically active single chain nanoparticles, *Macromolecules*, 2022, **55**, 9918–9924.
32 N. D. Knöfel, H. Rothfuss, P. Tzvetkova, B. Kulendran, C. Barner-Kowollik and P. W. Roesky, Heterobimetallic Eu(III)/Pt(II) single-chain nanoparticles: a path to enlighten catalytic reactions, *Chem. Sci.*, 2020, **11**, 10331–10336.
33 N. D. Knöfel, H. Rothfuss, C. Barner-Kowollik and P. W. Roesky, M-2(4+) paddlewheel clusters as junction points in single-chain nanoparticles, *Polym. Chem.*, 2019, **10**, 86–93.
34 J. Willenbacher, O. Altintas, V. Trouillet, N. Knöfel, M. J. Monteiro, P. W. Roesky and C. Barner-Kowollik, Pd-complex driven formation of single-chain nanoparticles, *Polym. Chem.*, 2015, **6**, 4358–4365.
35 H. Rothfuss, N. D. Knöfel, P. Tzvetkova, N. C. Michenfelder, S. Baraban, A. N. Unterreiner, P. W. Roesky and C. Barner-Kowollik, Phenanthroline-A versatile ligand for advanced functional polymeric materials, *Chem.–Eur. J.*, 2018, **24**, 17475–17486.
36 N. D. Knöfel, H. Rothfuss, J. Willenbacher, C. Barner-Kowollik and P. W. Roesky, Platinum(II)-crosslinked single-chain nanoparticles: an approach towards recyclable homogeneous catalysts, *Angew. Chem., Int. Ed.*, 2017, **56**, 4950–4954.
37 H. Rothfuss, N. D. Knöfel, P. W. Roesky and C. Barner-Kowollik, Single-chain nanoparticles as catalytic nanoreactors, *J. Am. Chem. Soc.*, 2018, **140**, 5875–5881.
38 J. Willenbacher, O. Altintas, P. W. Roesky and C. Barner-Kowollik, Single-chain self-folding of synthetic polymers induced by metal-ligand complexation, *Macromol. Rapid Commun.*, 2014, **35**, 45–51.
39 I. Asenjo-Sanz, T. Claros, E. González, J. Pinacho-Olaciregui, E. Verde-Sesto and J. A. Pomposo, Significant effect of intra-chain distribution of catalytic sites on catalytic activity in "clickase" single-chain nanoparticles, *Mater. Lett.*, 2021, **304**, 130622.
40 B. F. Patenaude, E. B. Berda and S. Pazicni, Probing secondary coordination sphere interactions within porphyrin-cored polymer nanoparticles, *Polym. Chem.*, 2022, **13**, 677–683.
41 A. Sathyan, S. Croke, A. M. Pérez-López, B. F. M. de Waal, A. Unciti-Broceta and A. R. A. Palmans, Developing Pd(II) based amphiphilic polymeric nanoparticles for pro-drug activation in complex media, *Mol. Syst. Des. Eng.*, 2022, **7**, 1736–1748.
42 A. Sathyan, T. Loman, L. Deng and A. R. A. Palmans, Amphiphilic polymeric nanoparticles enable homogenous rhodium-catalysed NH insertion reactions in living cells, *Nanoscale*, 2023, **15**, 12710–12717.
43 T. M. Xiong, E. S. Garcia, J. Chen, L. Zhu, A. J. Alzona and S. C. Zimmerman, Enzyme-like catalysis by single chain nanoparticles that use transition metal cofactors, *Chem. Commun.*, 2022, **58**, 985–988.
44 Y. Liu, T. Pauloehrl, S. I. Presolski, L. Albertazzi, A. R. A. Palmans and E. W. Meijer, Modular synthetic platform for the construction of functional single-chain polymeric nanoparticles: from aqueous catalysis to photosensitization, *J. Am. Chem. Soc.*, 2015, **137**, 13096–13105.
45 D. Arena, E. Verde-Sesto, I. Rivilla and J. A. Pomposo, Artificial photosynthases: single-chain nanoparticles with manifold visible-light photocatalytic activity for challenging "in water" organic reactions, *J. Am. Chem. Soc.*, 2024, **146**, 14397–14403.
46 J. J. Piane, S. Huss, L. T. Alameda, S. J. Koehler, L. E. Chamberlain, M. J. Schubach, A. C. Hoover and E. Elacqua, Single-chain polymers as homogeneous oxidative photoredox catalysts, *J. Polym. Sci.*, 2021, **59**, 2867–2877.
47 M. Spicuzza, S. P. Gaikwad, S. Huss, A. A. Lee, C. V. Craescu, A. Griggs, J. Joseph, M. Puthenpurayil, W. Lin, C. Matarazzo, S. Baldwin, V. Perez, D. A. Rodriguez-Acevedo, J. R. Swierk and E. Elacqua, Visible-light-mediated Diels–Alder reactions under single-chain polymer confinement: investigating the role of the crosslinking moiety on catalyst activity, *Polym. Chem.*, 2024, **15**, 1833–1838.
48 S. Mavila, C. E. Diesendruck, S. Linde, L. Amir, R. Shikler and N. G. Lemcoff, Polycyclooctadiene complexes of rhodium(I): direct access to organometallic nanoparticles, *Angew. Chem., Int. Ed.*, 2013, **52**, 5767–5770.
49 J. Chen, K. Li, S. E. Bonson and S. C. Zimmerman, A bioorthogonal small molecule selective polymeric "clickase", *J. Am. Chem. Soc.*, 2020, **142**, 13966–13973.
50 K. Mundsinger, A. Izuagbe, B. T. Tuten, P. W. Roesky and C. Barner-Kowollik, Single chain nanoparticles in catalysis, *Angew. Chem., Int. Ed.*, 2024, **63**, e202311734.
51 J. Rubio-Cervilla, E. González and J. A. Pomposo, Advances in single-chain nanoparticles for catalysis applications, *Nanomaterials*, 2017, **7**, 341.
52 M. B. Plutschack, B. Pieber, K. Gilmore and P. H. Seeberger, The hitchhiker's guide to flow chemistry, *Chem. Rev.*, 2017, **117**, 11796–11893.
53 D. T. McQuade and P. H. Seeberger, Applying flow chemistry: methods, materials, and multistep synthesis, *J. Org. Chem.*, 2013, **78**, 6384–6389.
54 L. D. Elliott, J. P. Knowles, P. J. Koovits, K. G. Maskill, M. J. Ralph, G. Lejeune, L. J. Edwards, R. I. Robinson,

 

I. R. Clemens, B. Cox, D. D. Pascoe, G. Koch, M. Eberle, M. B. Berry and K. I. Booker-Milburn, Batch *versus* flow photochemistry: a revealing comparison of yield and productivity, *Chem.–Eur. J.*, 2014, **20**, 15226–15232.

55 D. J. Walsh, D. A. Schinski, R. A. Schneider and D. Guironnet, General route to design polymer molecular weight distributions through flow chemistry, *Nat. Commun.*, 2020, **11**, 3094.

56 M. H. Reis, F. A. Leibfarth and L. M. Pitet, Polymerizations in continuous flow: recent advances in the synthesis of diverse polymeric materials, *ACS Macro Lett.*, 2020, **9**, 123–133.

57 M. Van De Walle, K. De Bruycker, J. P. Blinco and C. Barner-Kowollik, Two colour photoflow chemistry for macromolecular design, *Angew. Chem., Int. Ed.*, 2020, **59**, 14143–14147.

58 O. Galant, H. B. Donmez, C. Barner-Kowollik and C. E. Diesendruck, Flow photochemistry for single-chain polymer nanoparticle synthesis, *Angew. Chem., Int. Ed.*, 2021, **60**, 2042–2046.

59 P. H. Maag, F. Feist, V. X. Truong, H. Frisch, P. W. Roesky and C. Barner-Kowollik, Visible-light-induced control over reversible single-chain nanoparticle folding, *Angew. Chem., Int. Ed.*, 2023, **62**, e202309259.

60 H. Frisch, F. R. Bloesser and C. Barner-Kowollik, Controlling chain coupling and single-chain ligation by two colours of visible light, *Angew. Chem., Int. Ed.*, 2019, **58**, 3604–3609.

61 T. S. Fischer, S. Spann, Q. An, B. Luy, M. Tsotsalas, J. P. Blinco, H. Mutlu and C. Barner-Kowollik, Self-reporting and refoldable profluorescent single-chain nanoparticles, *Chem. Sci.*, 2018, **9**, 4696–4702.

62 D. Kodura, H. A. Houck, F. R. Bloesser, A. S. Goldmann, F. E. Du Prez, H. Frisch and C. Barner-Kowollik, Light-fueled dynamic covalent crosslinking of single polymer chains in non-equilibrium states, *Chem. Sci.*, 2021, **12**, 1302–1310.

63 J. A. Barltrop and P. Schofield, Photosensitive protecting groups, *Tetrahedron Lett.*, 1962, **3**, 697–699.

64 D. H. R. Barton, Y. L. Chow, A. Cox and G. W. Kirby, 654. Photochemical transformations. Part XIX. Some photosensitive protecting groups, *J. Chem. Soc.*, 1965, 3571–3578, DOI: **10.1039/JR9650003571**.

65 D. H. R. Barton, Y. L. Chow, A. Cox and G. W. Kirby, Photosensitive protection of functional groups, *Tetrahedron Lett.*, 1962, **3**, 1055–1057.

66 A. Patchornik, B. Amit and R. Woodward, Photosensitive protecting groups, *J. Am. Chem. Soc.*, 1970, **92**, 6333–6335.

67 J. C. Sheehan and R. M. Wilson, Photolysis of desyl compounds. A new photolytic cyclization, *J. Am. Chem. Soc.*, 1964, **86**, 5277–5281.

68 P. Klán, T. Šolomek, C. G. Bochet, A. Blanc, R. Givens, M. Rubina, V. Popik, A. Kostikov and J. Wirz, Photoremovable protecting groups in chemistry and biology: reaction mechanisms and efficacy, *Chem. Rev.*, 2013, **113**, 119–191.

69 H. Zhao, E. S. Sterner, E. B. Coughlin and P. Theato, o-Nitrobenzyl alcohol derivatives: opportunities in polymer and materials science, *Macromolecules*, 2012, **45**, 1723–1736.

70 E. J. Foster, E. B. Berda and E. W. Meijer, Metastable supramolecular polymer nanoparticles *via* intramolecular collapse of single polymer chains, *J. Am. Chem. Soc.*, 2009, **131**, 6964–6966.

71 I. M. Irshadeen, S. L. Walden, M. Wegener, V. X. Truong, H. Frisch, J. P. Blinco and C. Barner-Kowollik, Action plots in action: in-depth insights into photochemical reactivity, *J. Am. Chem. Soc.*, 2021, **143**, 21113–21126.

72 S. L. Walden, J. A. Carroll, A.-N. Unterreiner and C. Barner-Kowollik, Photochemical action plots reveal the fundamental mismatch between absorptivity and photochemical reactivity, *Adv. Sci.*, 2024, **11**, 2306014.

73 C. Yao, X. Wang, G. Liu, J. Hu and S. Liu, Distinct morphological transitions of photoreactive and thermoresponsive vesicles for controlled release and nanoreactors, *Macromolecules*, 2016, **49**, 8282–8295.

74 N. De Alwis Watuthanthrige, P. N. Kurek and D. Konkolewicz, Photolabile protecting groups: a strategy for making primary amine polymers by RAFT, *Polym. Chem.*, 2018, **9**, 1557–1561.

75 X. Wang, G. Liu, J. Hu, G. Zhang and S. Liu, Concurrent block copolymer polymersome stabilization and bilayer permeabilization by stimuli-regulated "traceless" crosslinking, *Angew. Chem., Int. Ed.*, 2014, **53**, 3138–3142.

76 J. Bachmann, C. Petit, L. Michalek, Y. Catel, E. Blasco, J. P. Blinco, A.-N. Unterreiner and C. Barner-Kowollik, Chain-length-dependent photolysis of ortho-nitrobenzyl-centered polymers, *ACS Macro Lett.*, 2021, **10**, 447–452.

77 C. Petit, J. Bachmann, L. Michalek, Y. Catel, E. Blasco, J. P. Blinco, A.-N. Unterreiner and C. Barner-Kowollik, UV-induced photolysis of polyurethanes, *Chem. Commun.*, 2021, **57**, 2911–2914.

78 S. Perrier, 50th Anniversary perspective: RAFT polymerization—A user guide, *Macromolecules*, 2017, **50**, 7433–7447.

79 H. A. Jahn and E. Teller, Stability of polyatomic molecules in degenerate electronic states. I. Orbital degeneracy, *Proc. R. Soc. A*, 1937, **161**, 220–235.

80 S. Li, D. Tian, X. Zhao, Y. Yin, R. Lee and Z. Jiang, Visible light-driven copper(II) catalyzed aerobic oxidative cleavage of carbon–carbon bonds: a combined experimental and theoretical study, *Org. Chem. Front.*, 2022, **9**, 6229–6239.

81 K. Mundsinger, B. T. Tuten, L. Wang, K. Neubauer, C. Kropf, M. L. O'Mara and C. Barner-Kowollik, Visible-light-reactive single-chain nanoparticles, *Angew. Chem., Int. Ed.*, 2023, **62**, e202302995.

82 S. Mavila, I. Rozenberg and N. G. Lemcoff, A general approach to mono- and bimetallic organometallic nanoparticles, *Chem. Sci.*, 2014, **5**, 4196–4203.

83 J. A. Pomposo, A. J. Moreno, A. Arbe and J. Colmenero, Local domain size in single-chain polymer nanoparticles, *ACS Omega*, 2018, **3**, 8648–8654.

84 A. Sanchez-Sanchez, A. Arbe, J. Colmenero and J. A. Pomposo, Metallo-folded single-chain nanoparticles with catalytic selectivity, *ACS Macro Lett.*, 2014, **3**, 439–443.

85 S. Tshepelevitsh, A. Kütt, M. Lõkov, I. Kaljurand, J. Saame, A. Heering, P. G. Plieger, R. Vianello and I. Leito, On the

basicity of organic bases in different media, *Eur. J. Org Chem.*, 2019, **2019**, 6735–6748.
86 A. Kütt, S. Tshepelevitsh, J. Saame, M. Lõkov, I. Kaljurand, S. Selberg and I. Leito, Strengths of acids in acetonitrile, *Eur. J. Org. Chem.*, 2021, **2021**, 1407–1419.
87 J. F. Coetzee, Ionic reactions in acetonitrile, *Prog. Phys. Org. Chem.*, 1967, **4**, 45–92.
88 A. Kütt, I. Leito, I. Kaljurand, L. Sooväli, V. M. Vlasov, L. M. Yagupolskii and I. A. Koppel, A comprehensive self-consistent spectrophotometric acidity scale of neutral brønsted acids in acetonitrile, *J. Org. Chem.*, 2006, **71**, 2829–2838.
89 A.-L. Fameau and T. Zemb, Self-assembly of fatty acids in the presence of amines and cationic components, *Adv. Colloid Interface Sci.*, 2014, **207**, 43–64.